

Cite this: *Polym. Chem.*, 2025, **16**,  
1365

# Preparation of phenyl-substituted open-cage silsesquioxane-pendant polysiloxanes and their thermal and optical properties†

Miku Kosaka,<sup>a</sup> Kenji Kanaori,<sup>a</sup> Hiroaki Imoto <sup>a</sup> and Kensuke Naka <sup>\*a,b</sup>

We prepared phenyl-substituted corner-opened type polyhedral oligomeric silsesquioxanes (CO-POSSs) bearing tris(dimethoxysilyl)-groups with variable linker lengths at the opening vertex; that is, tris(dimethoxysilyl-ethyl-dimethylsiloxy)- and tris(dimethoxysilyl-propylthioethyl-dimethylsiloxy)-heptaphenyl-substituted CO-POSSs (**Ph-H** and **Ph-V**). Optically transparent free-standing films of phenyl-substituted open-cage silsesquioxane-pendant polysiloxanes (**PolyPh-H**) were prepared by optimizing the sol-gel reaction conditions for **Ph-H**. Polycondensation of **Ph-V** afforded an optically transparent and flexible phenyl-substituted CO-POSS-pendant polysiloxane film (**PolyPh-V**). The polycondensations of **Ph-H** and **Ph-V** were fully completed even at 50 °C for 6 h under vacuum. <sup>29</sup>Si cross-polarization magic angle spinning (CP-MAS) NMR analysis suggests that the films included cyclotrisiloxane (D<sub>3</sub>) and linear siloxane (D<sub>linear</sub>) structures. The effects of the polysiloxane structures on the thermal and mechanical properties were studied. The highest temperature at which the sample lost 5 wt% of the original mass (*T*<sub>d5</sub>) under N<sub>2</sub> (381 °C) was obtained for **PolyPh-V**, even though it contained a flexible linker unit. The predominant linear siloxane structures may provide increase higher thermal stability. The UV-vis spectra of the resulting transparent films were mostly unchanged even after six days of exposure to UV irradiation in air. The present study shows that phenyl-substituted CO-POSS-pendant polysiloxanes represent alternative UV-resistant, optically transparent materials with higher heat resistance.

Received 21st December 2024,  
Accepted 10th February 2025

DOI: 10.1039/d4py01460j

rsc.li/polymers

## Introduction

Silicone resins derived from hydrolysis and condensation reactions of alkoxy silanes and chlorosilanes are industrially important organic-inorganic hybrid materials due to their superior thermal, mechanical, optical, and electrical properties.<sup>1,2</sup> Combinations of various siloxane monomeric units are indicated using “M” (R<sub>3</sub>SiO<sub>0.5</sub>), “D” (R<sub>2</sub>SiO), “T” (RSiO<sub>1.5</sub>), and “Q” (SiO<sub>2</sub>), with a wide variety of organic substituents offering a broad range of material properties. With the increasing performance of electronic devices and power electronics, the development of multifunctional silicone materials that are optically transparent and can be obtained with low processing temperatures is an important task.<sup>3–5</sup> Depending on their

purpose, such materials require several properties to be combined, including high thermal conductivity, insulation, heat resistance, UV resistance, flexibility, high refractive index, and lightweight character. These requirements often have a trade-off relationship, and trial-and-error studies are typically required to combine these characteristics. The usual sol-gel reaction that is used to obtain silicone resins requires a high-curing temperature to facilitate the condensation reaction. However, unreacted alkoxy and silanol groups can remain, which affect the physical properties and functions of the materials, and complete consumption is difficult to achieve under typical sol-gel reaction condition.<sup>5,6</sup> In addition, although the molecular level structures of the siloxane linkages significantly affect the physical properties of the materials, controlling the structures of silicone resins at the molecular level is difficult with standard sol-gel processing.<sup>7–9</sup> Correlations between three-dimensional well-defined molecular-level structures and bulk properties remain unclear.

To address these issues, the concept of “polymeric materials based on element-blocks” is expected to facilitate new research and lead to new ideas for materials design with well-defined molecular-level structures in three-dimensions.<sup>10</sup> Polyhedral oligomeric silsesquioxanes (POSSs), particularly,

<sup>a</sup>Faculty of Molecular Chemistry and Engineering, Graduate School of Science and Technology, Kyoto Institute of Technology, Kyoto 606-8585, Japan.

E-mail: kenaka@kit.ac.jp

<sup>b</sup>Materials Innovation Lab, Kyoto Institute of Technology, Goshokaido-cho, Matsugasaki, Sakyo-ku, Kyoto 606-8585, Japan

†Electronic supplementary information (ESI) available: NMR spectra, MALDI-TOF-MS spectra, FT-IR spectra, DSC and DMA analyses. See DOI: <https://doi.org/10.1039/d4py01460j>



cage octasilsesquioxanes ( $T_8$  cages), have attracted growing interest over the past several decades as well-defined and important element-blocks.<sup>11,12</sup> The use of POSS derivatives as monomers provides an attractive approach to the design of organic–inorganic hybrid polymers. Among the POSS family, open-cage silsesquioxanes; that is, incompletely condensed POSSs (IC-POSSs), represent promising element-blocks for building organic–inorganic hybrid materials.<sup>13</sup> Corner-opened type POSSs (CO-POSS), termed trisilanols, are easily prepared *via* a one-step reaction from the corresponding silane coupling agents. One of the advantages of CO-POSSs is that variations in substituents such as isobutyl, phenyl, trifluoropropyl, and cyclohexyl groups at the seven Si corners are possible, and various functional groups can be easily introduced to the opened moiety of the CO-POSSs. Compared to completely condensed POSSs, while their thermal stabilities are comparable, the crystallinity of CO-POSSs is significantly reduced due to their reduced symmetry.<sup>13</sup> CO-POSS is a suitable backbone for cross-linking agents in network polymers because three reactive sites can be easily introduced into their open moieties.<sup>14–16</sup> Trisilanols are also suitable monomers for double cyclopolymerization because three functional groups are configured in the axial position and fixed in one direction.<sup>17</sup> Previously, we designed trifluoropropyl-substituted CO-POSS bearing tris(dimethoxysilyl) groups and found that trifluoropropyl-substituted CO-POSS-pendant polysiloxanes were obtained by hydrolysis and polycondensation under mild conditions; that is, the polycondensation of the starting materials was fully achieved even at 50 °C within 6 h.<sup>18,19</sup> These materials can be seen as DT resins with well-defined three-dimensional molecular-level structures. The resulting films exhibit excellent UV resistance, good flexibility, and optical transparency.

The properties of POSS compounds such as their crystallinity, solubility, compatibility, and thermal behavior are highly dependent on the type of organic substituents they harbor. Among them, phenyl-substituted POSS structures have higher thermal stability than saturated aliphatic POSSs, and such materials generally have a higher refractive index.<sup>20</sup> Here, we prepared tris(dimethoxysilyl-ethyl-dimethylsiloxy)- and tris(dimethoxysilyl-propylthioethyl-dimethylsiloxy)-heptaphenyl-substituted CO-POSSs (**Ph-H** and **Ph-V**, respectively) as phenyl-substituted CO-POSS derivatives with tris(dimethoxysilyl)-groups. We optimized the sol–gel reaction to obtain free-standing films of the phenyl-substituted CO-POSS-pendant polysiloxanes. We found that the polycondensation proceeded to completion without any unreacted silanol groups in a low-temperature solution process at 50 °C for 6 h under vacuum. The effects of the polysiloxane structures on the thermal and mechanical properties were also studied.

## Results and discussion

Ethylene-linked tris(dimethoxysilyl)-heptaphenyl-substituted open-cage silsesquioxane (**Ph-H**) was prepared *via* hydrosilyl-

ation of 3,7,14-tris(dimethylsilyloxy)heptaphenyltricycloheptasiloxane with dimethoxymethylvinylsilane (Fig. S1†). The dimethoxysilyl groups of **Ph-H** were hydrolyzed with 1 M HCl in THF (Scheme 1). After concentrated the reaction mixture under reduced pressure, the complete hydrolysis of the methoxy groups in **Ph-H** was confirmed by <sup>1</sup>H NMR analysis of the residual products (Fig. S2a†). The residues were then re-dissolved in THF and the sol solution was cast onto a substrate, air-dried for one day, and fully condensed at 50 °C for 6 h under reduced pressure to afford phenyl-substituted CO-POSS-pendant polysiloxane films (**PolyPh-H**). When the concentration of the re-dissolved hydrolyzed material in THF was 0.16 g mL<sup>-1</sup>, only a fragile film of **PolyPh-H<sup>a</sup>** was obtained and the resulting product was difficult to peel from the substrate (Fig. 1A). On the other hand, when the re-dissolved concentration of hydrolyzed **Ph-H** was increased to 0.88 g mL<sup>-1</sup> gave a transparent, rigid, free-standing film of **PolyPh-H<sup>b</sup>** (Fig. 1B). With the same concentration, when the condensation temperature was increased to 100 °C for 6 h, **PolyPh-H<sup>c</sup>** was formed as a fragile film (Fig. 1C). Although **PolyPh-H<sup>a</sup>** and **PolyPh-H<sup>c</sup>** were partially soluble in acetone, chloroform, and THF, **PolyPh-H<sup>b</sup>** was insoluble in these organic solvents. The optical transmittances of all the films were over 97% in the visible region (Fig. S3†).

<sup>29</sup>Si cross-polarization magic-angle spinning (CP-MAS) NMR analysis of **PolyPh-H<sup>a</sup>**, **PolyPh-H<sup>b</sup>**, and **PolyPh-H<sup>c</sup>**, showed characteristic resonance peaks at 9 ppm and between –66 and –75 ppm corresponding to the M units, (CH<sub>3</sub>)<sub>2</sub>(SiO<sub>0.5</sub>)X, and T units, CF<sub>3</sub>CH<sub>2</sub>CH<sub>2</sub>(SiO<sub>1.5</sub>), in the CO-POSS structure, respect-



**Scheme 1** Preparation of phenyl-substituted open-cage silsesquioxane-pendant polysiloxane **PolyPh-H** from **Ph-H**.

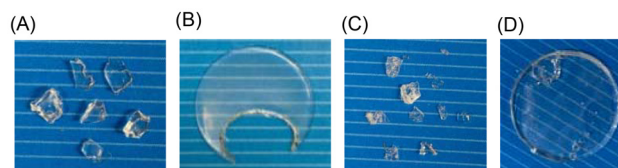


**Fig. 1** Appearances of (A) **PolyPh-H<sup>a</sup>**, (B) **PolyPh-H<sup>b</sup>**, (C) **PolyPh-H<sup>c</sup>**, and (D) **PolyPh-V**.





Fig. 2  $^{29}\text{Si}$  CP-MAS (119 MHz) NMR spectra for PolyPh-H<sup>a</sup>, PolyPh-H<sup>b</sup>, PolyPh-H<sup>c</sup>, and PolyPh-V. The insert shows the content ratio of the D<sub>3</sub> and D<sub>linear</sub> units against the total D unit according to the integral ratio.

ively (Fig. 2). The results confirmed that the  $-\text{SiOMe}$  and  $\text{SiOH}$  groups, which should be observed at  $-0.61$  ppm and  $-4.64$  ppm, respectively, were absent, indicating complete polycondensation. Furthermore, no adsorption at around  $2835\text{ cm}^{-1}$  or  $3625\text{ cm}^{-1}$  corresponding to the  $-\text{SiOMe}$  and  $\text{SiOH}$  groups, respectively, was observed in the Fourier-transform infrared (FT-IR) spectra of the condensed products (Fig. S4<sup>†</sup>), which also indicated that condensation was complete even at  $50\text{ }^\circ\text{C}$ . No detectable adsorption derived from the  $-\text{SiOH}$  groups in the FT-IR analysis after storage for three months at room temperature (Fig. S5<sup>†</sup>). The  $^{29}\text{Si}$  CP-MAS NMR spectra of the films also included two new peaks at approximately  $-10$  and  $-20$  ppm ascribed to D units formed upon polycondensation. These peaks were attributed to cyclotrisiloxane structure (D<sub>3</sub>) and linear siloxane structures (D<sub>linear</sub>), respectively.<sup>21,22</sup> Sample PolyPh-H<sup>a</sup> exhibited predominant peaks at  $-10$  ppm, corresponding to the D<sub>3</sub> structure. The content ratio of the D<sub>linear</sub> to the total D units was 28% according to the integral ratio. Increasing the concentration of hydrolyzed Ph-H to  $0.88\text{ g mL}^{-1}$  led to a decrease in the signal at  $-10$  ppm and an increase in the signal at  $-25$  ppm. The intensity ratio of the linear siloxane structures relative to the total D units in PolyPh-H<sup>b</sup> increased to 39%. Increasing the condensation temperature to  $100\text{ }^\circ\text{C}$  for PolyPh-H<sup>c</sup>, led to a decrease in the content of the linear siloxane structure to 31%. Decreasing the content of the linear siloxane structures may inhibit the formation of the free-standing-films.

The dimethoxysilyl groups of the propylenethioethyl-linked tris(dimethoxysilyl)-heptaphenyl-substituted CO-POSS (Ph-V) (Fig. S6<sup>†</sup>) were also hydrolyzed and partially condensed with 1 M HCl in THF (Scheme 2). The reaction solution was then concentrated, and the residual products were re-dissolved in THF



Scheme 2 Preparation of phenyl-substituted open-cage silsesquioxane-pendant polysiloxane (PolyPh-V) from Ph-V.

to a concentration of  $0.88\text{ g mL}^{-1}$ . Subsequently, the sol solution was cast onto a substrate, air-dried for one day, and fully condensed at different temperatures under reduced pressure for polycondensation to afford an optically transparent and flexible phenyl-substituted CO-POSS-pendant polysiloxane film (PolyPh-V) (Fig. 1D). The  $^{29}\text{Si}$  CP-MAS NMR spectrum of the film PolyPh-V showed predominantly peaks at  $-25$  ppm, corresponding to the linear siloxane structure. The intensity ratio of the linear siloxane structures relative to the total D units was 64%. Complete polycondensation and the absence of  $-\text{SiOMe}$  and  $\text{SiOH}$  groups were confirmed (Fig. 2 and S4<sup>†</sup>). The resulting freestanding film was sufficiently flexible to bend without cracking. The sample of PolyPh-V was insoluble in common organic solvents. SEM analysis of PolyPh-V showed smooth surface and no aggregation in the order of several micrometers (Fig. S7<sup>†</sup>).

The densities of PolyPh-H<sup>a</sup>, PolyPh-H<sup>b</sup>, PolyPh-H<sup>c</sup> were  $1.2132 \pm 0.0046\text{ g cm}^{-3}$ ,  $1.2220 \pm 0.0031\text{ g cm}^{-3}$ , and  $1.233 \pm 0.005\text{ g cm}^{-3}$ , respectively, based on gas displacement pycnometry analysis (Table 1). The higher density of PolyPh-H<sup>b</sup> compared to that of PolyPh-H<sup>a</sup> suggests that a greater proportion of linear units increased the density of the material. Furthermore, the higher density of PolyPh-H<sup>c</sup> than those of the other materials, suggests that higher curing temperatures also increased the density. The density of PolyPh-V ( $1.2019 \pm 0.005\text{ g cm}^{-3}$ ) was lower than those of PolyPh-H due to the increase in the organic content.

The thermal stabilities of all the products were estimated from thermogravimetric analysis (TGA) data obtained under  $\text{N}_2$  (Fig. 3). The temperatures at which samples of PolyPh-H<sup>a</sup>, PolyPh-H<sup>b</sup>, PolyPh-H<sup>c</sup>, and PolyPh-V lost 5 wt% of their original mass ( $T_{d5}$ ) under  $\text{N}_2$  were  $360$ ,  $366$ ,  $376$   $^\circ\text{C}$ , and  $381$   $^\circ\text{C}$ , respectively. The  $T_{d5}$  values for PolyPh-H were correlated with the density. Even considering the presence of the flexible linker unit, the highest  $T_{d5}$  value was obtained for PolyPh-V. In this case, predominant linear siloxane structures may provide increase higher thermal stability.

Differential scanning calorimetry (DSC) analysis of PolyPh-H<sup>a</sup>, PolyPh-H<sup>b</sup>, and PolyPh-H<sup>c</sup> revealed glass transition temp-



**Table 1** Density ( $\rho$ ), specific heat ( $C_p$ ), thermal diffusivity ( $\alpha$ ), and thermal conductivities ( $\lambda$ ) of the samples

| Sample                      | $\rho^a$ (kg cm <sup>-3</sup> )   | $C_p^b$ (J (kg K) <sup>-1</sup> ) | $\alpha^c$ (m <sup>2</sup> s <sup>-1</sup> ) | $\lambda$ (W (m K) <sup>-1</sup> ) |
|-----------------------------|-----------------------------------|-----------------------------------|--|------------------------------------|
| <b>PolyPh-H<sup>a</sup></b> | $(1.2132 \pm 0.0046) \times 10^3$ | $(1.37 \pm 0.05) \times 10^3$     | $(0.89 \pm 0.06) \times 10^{-7}$             | $0.15 \pm 0.01$                    |
| <b>PolyPh-H<sup>b</sup></b> | $(1.2220 \pm 0.0031) \times 10^3$ | $(1.37 \pm 0.01) \times 10^3$     | $(1.30 \pm 0.20) \times 10^{-7}$             | $0.22 \pm 0.03$                    |
| <b>PolyPh-H<sup>c</sup></b> | $(1.2330 \pm 0.0050) \times 10^3$ | $(1.18 \pm 0.03) \times 10^3$     | $(0.80 \pm 0.30) \times 10^{-7}$             | $0.12 \pm 0.04$                    |
| <b>PolyPh-V</b>             | $(1.2019 \pm 0.0013) \times 10^3$ | $(1.19 \pm 0.02) \times 10^3$     | $(0.99 \pm 0.08) \times 10^{-7}$             | $0.14 \pm 0.01$                    |
| <b>Ran-B</b>                | $(1.2075 \pm 0.0009) \times 10^3$ | $(1.30 \pm 0.06) \times 10^3$     | $(1.07 \pm 0.03) \times 10^{-7}$             | $0.17 \pm 0.01$                    |
| <b>PolyF-H</b>              | $(1.3765 \pm 0.0036) \times 10^3$ | $(1.12 \pm 0.02) \times 10^3$     | $(0.80 \pm 0.02) \times 10^{-7}$             | $0.12 \pm 0.004$                   |
| <b>PolyB-H</b>              | $(1.0843 \pm 0.0036) \times 10^3$ | $(1.45 \pm 0.02) \times 10^3$     | $(0.77 \pm 0.06) \times 10^{-7}$             | $0.12 \pm 0.01$                    |

<sup>a</sup> Average values of ten independent measurements. <sup>b</sup> Average values of three independent measurements. <sup>c</sup> Average of two independent film productions and five measurements for each film.

**Fig. 3** TGA thermograms of **PolyPh-H<sup>a</sup>**, **PolyPh-H<sup>b</sup>**, **PolyPh-H<sup>c</sup>**, and **PolyPh-V** at a heating rate of 10 °C min<sup>-1</sup> in N<sub>2</sub> flow.

eratures ( $T_g$ ) under N<sub>2</sub> of 67, 73, and 82 °C, respectively (Fig. S8†). The  $T_g$  values for **PolyPh-H** also correlated with the density. DSC analysis of **PolyPh-V** revealed a  $T_g$  value under N<sub>2</sub> of 54 °C. No softening was observed above the  $T_g$  for **PolyPh-H<sup>a</sup>**, **PolyPh-H<sup>b</sup>**, and **PolyPh-H<sup>c</sup>**, whereas softening of **PolyPh-V** was observed above its  $T_g$ . Dynamic mechanical analysis (DMA) measurements were performed on the freestanding films of **PolyPh-V** (Fig. S9†) showed that the  $T_g$  was manifested as a gentle step in  $E'$ , a broad peak in  $E''$ , and a clear peak in  $\tan \delta$ . The measured  $T_g$  was consistent with that of the  $T_g$  observed in the DSC analysis.

Thermal conductivities ( $\lambda$ ) of the films were calculated by multiplying the corresponding thermal diffusivity ( $\alpha$ ), density ( $\rho$ ), and specific heat ( $C_p$ ); the results for all the tested films are summarized in Table 1. The highest thermal conductivity of 0.22 W m<sup>-1</sup> K<sup>-1</sup> was observed for **PolyPh-H<sup>b</sup>**, with **PolyPh-H<sup>a</sup>** and **PolyPh-H<sup>c</sup>** showing lower thermal conductivities. Increasing the number of linear siloxane structures thus increased the thermal conductivity, especially the thermal diffusivity. A higher thermal diffusivity was observed for **PolyPh-V**, which may be due to the predominant content of linear siloxane structures. Decreasing the density and volumetric heat capacity reduced the thermal conductivity of **PolyPh-V**.

To study the effect of the CO-POSS structure, random polysilsesquioxanes were prepared from 1-(methyldimethoxysilyl)-2-(dimethylmethoxysilyl)ethane (MDME) and phenyltrimethoxysilane (PTMS) using the same components and conditions used for **1** with a MDME/PTMS molar ratio of 3 : 7, *via* hydrolysis and condensation performed under the same conditions as those used to generate **PolyPh-H<sup>b</sup>** and **PolyPh-H<sup>c</sup>** (Scheme 3). The reaction solution was concentrated, and the residual product was re-dissolved in THF to 0.88 g mL<sup>-1</sup> and then condensed at either 50 °C for 6 h or 100 °C for 6 h to afford **Ran-A** and **Ran-B**, respectively. TGA analysis of **Ran-A** and **Ran-B** revealed  $T_{d5}$  values of 249 and 279 °C, respectively (Fig. S10†). Increasing the condensation temperature increased the  $T_{d5}$  value. This low condensation temperature resulted in unreacted alkoxy groups and silanol groups remaining, thereby reducing the thermal stability. The density of **Ran-B** ( $1.2075 \pm 0.0009$  g cm<sup>-3</sup>) was lower than that of **PolyPh-H<sup>b</sup>**. The CO-POSS based-structure promoted complete polycondensation without -SiOMe and SiOH groups. A higher thermal diffusivity was observed for **Ran-B** than for **PolyPh-H<sup>a</sup>** and **PolyPh-H<sup>c</sup>**, but lower than that for **PolyPh-H<sup>b</sup>**.

Tris(dimethoxysilyl-ethyl-dimethylsiloxy)-heptatrifluoropropyl-substituted open-cage silsesquioxane (**F-H**) (Fig. 4) and tris(dimethoxysilyl-ethyl-dimethylsiloxy)-heptaisobutyl-substituted open-cage silsesquioxane (**B-H**) were hydrolyzed and condensed to afford isobutyl- and trifluoropropyl-substituted open-cage silsesquioxane-pendant polysiloxanes **PolyF-H** and **PolyB-H** under the same conditions as **PolyPh-H**, except using toluene in the case of **PolyB-H**. The relative intensity ratios of the linear siloxane structures to the total D units are 52% for **PolyF-H** and 62% for **PolyB-H**, respectively (Fig. S11†). The thermal conductivities and thermal diffusivities were lower than those of **PolyPh-H<sup>b</sup>**.

**Scheme 3** Synthesis of random polysilsesquioxanes (**Ran-A** and **Ran-B**) from 1-(methyldimethoxysilyl)-2-(dimethylmethoxysilyl)ethane (MDME) and phenyltrimethoxysilane (PTMS).



Fig. 4 Chemical structures of F-H and B-H.

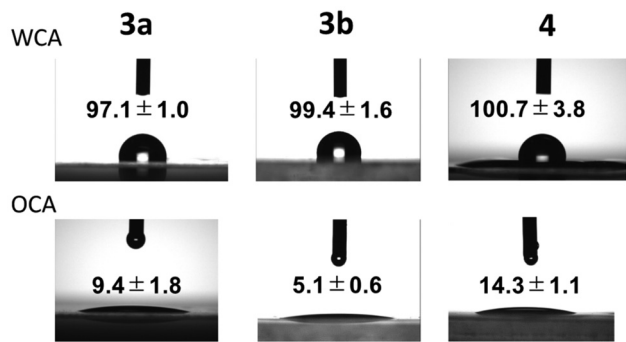


Fig. 5 Static water and *n*-tetradecane contact angles of the films of PolyPh-H<sup>a</sup>, PolyPh-H<sup>b</sup>, and PolyPh-V.

The surface hydrophobicity of the films was investigated by static contact angle measurements with probe liquids such as water ( $\theta_{\text{water}}$ ) and *n*-tetradecane ( $\theta_{n\text{-tetradecane}}$ ) (Fig. 5). The contact angle for PolyPh-H<sup>c</sup> was difficult to assess because of its many cracks. The water contact angles of PolyPh-H<sup>a</sup>, PolyPh-H<sup>b</sup>, and PolyPh-V were 97.1°, 99.4°, and 100.7°, respectively. *n*-Tetradecane contact angles of PolyPh-H<sup>a</sup>, PolyPh-H<sup>b</sup>, and PolyPh-V were 9.4°, 5.1°, and 14.3°, respectively. The surface free energies of the cast films were estimated using the geometric mean model described by eqn (1) and (2):

$$1 + \cos \theta = (2/\gamma_L)[(\gamma_L^d \gamma_s^d)^{0.5} + (\gamma_L^p \gamma_s^p)^{0.5}] \quad (1)$$

$$\gamma_s^d + \gamma_s^p = \gamma_s \quad (2)$$

where  $\theta$  is the static contact angle;  $\gamma_L$  and  $\gamma_s$  are the surface free energies of liquid and solid, respectively; and  $\gamma^d$  and  $\gamma^p$  are dispersive and polar components of  $\gamma$ , respectively. No significant difference of the surface free energies of PolyPh-H<sup>a</sup> and PolyPh-H<sup>b</sup> was observed, even their bulk properties were different.

A solubility study of isobutyl- and phenyl-substituted T<sub>8</sub> cages suggested that the bulky isobutyl groups were completely covered by the polar siloxane cage framework.<sup>2,3</sup> In contrast, part of the polar siloxane cage framework was exposed to the environment for derivatives with phenyl substituents. In this study, the surface free energies of PolyPh-H<sup>a</sup>, PolyPh-H<sup>b</sup>, and PolyPh-V were higher than those of PolyF-H and PolyB-H (Table 2). The surface free energy of Ran-A was lower than those of PolyPh-H<sup>a</sup> and PolyPh-H<sup>b</sup>, suggesting that the siloxane

Table 2 Static contact angles and surface free energies

| Sample                | Static contact angles (°) |                                 | Surface free energy <sup>a</sup> (mN m <sup>-1</sup> ) |              |            |
|-----------------------|---------------------------|---------------------------------|--|--------------|------------|
|                       | $\theta_{\text{water}}$   | $\theta_{n\text{-tetradecane}}$ | $\gamma_s^d$   | $\gamma_s^p$ | $\gamma_s$ |
| PolyPh-H <sup>a</sup> | 97.1 ± 1.0                | 9.4 ± 1.8                       | 26.0   | 0.7          | 26.7       |
| PolyPh-H <sup>b</sup> | 99.4 ± 1.6                | 5.1 ± 0.6                       | 26.3   | 0.4          | 26.7       |
| PolyPh-V              | 100.7 ± 3.8               | 14.3 ± 1.1                      | 25.6   | 0.3          | 25.9       |
| Ran-A                 | 98.0 ± 0.5                | 21.7 ± 0.7                      | 24.6   | 0.7          | 25.3       |
| PolyF-H               | 96.2 ± 2.3                | 31.3 ± 4.1                      | 22.7   | 1.4          | 24.1       |
| PolyB-H               | 98.7 ± 1.1                | 23.2 ± 1.2                      | 24.3   | 0.7          | 25.0       |

<sup>a</sup> Water:  $\gamma_{\text{water}}^d = 26.4 \text{ mN m}^{-1}$ ,  $\gamma_{\text{water}}^p = 46.4 \text{ mN m}^{-1}$ ; *n*-tetradecane:  $\gamma_{n\text{-tetradecane}}^d = 26.4 \text{ mN m}^{-1}$ ,  $\gamma_{n\text{-tetradecane}}^p = 0.0 \text{ mN m}^{-1}$ .



Fig. 6 Transmittance spectra of (A) PolyPh-H<sup>b</sup>, and (B) PolyPh-V, along with UV irradiation time in air. The thicknesses were within 39–75 μm.

backbone in the cage structure with high curvature was more exposed than in the random type.

Transmittance spectra corresponding to varying irradiation times for PolyPh-H<sup>b</sup> were used to study the UV resistance in air (Fig. 6A). The initial transmittance spectrum of PolyPh-H<sup>b</sup> showed a high transmittance from 300 nm to 600 nm. No significant change in the transmittance was observed after PolyPh-H<sup>b</sup> was irradiated with 365 nm UV light for 6 days. It is known that organic substituents, such as methyl groups and unreacted residual alkoxy groups in siloxane absorb UV light and generate radicals,<sup>3,5</sup> this can result further oxidation and a reduction in transparency. Complete consumption of the alkoxy groups thus suppresses decomposition upon exposure to UV light. The transmittance of PolyPh-V at approximately 300 nm decreased upon exposure to UV irradiation for several days (Fig. 6B). The decrease in the transmittance at 300 nm was due to the absorption by sulfoxide formed by the oxidation of sulfur atoms. No decrease in the transmittance was observed at wavelength longer than 350 nm; thus 4 appeared colorless and transparent even after 6 days of UV irradiation.

## Conclusions

We prepared phenyl-substituted IC-POSSs bearing tris (dimethoxysilyl) groups at the open positions and optimized their sol-gel reactions to obtain optically transparent free-



standing films. Polycondensation was fully completed *via* a low-temperature solution process, even at 50 °C for 6 h under vacuum. The  $T_{d5}$  values under  $N_2$  for **PolyPh-H<sup>a</sup>**, **PolyPh-H<sup>b</sup>**, and **PolyPh-H<sup>c</sup>** (360, 366, and 376 °C, respectively) correlated with their densities. The highest  $T_{d5}$  value was obtained for **PolyPh-V**, even in the presence of the flexible linker unit. The predominant linear siloxane structures may provide increase higher thermal stability. The film of **PolyPh-H<sup>b</sup>** exhibited high optical transparency, heat resistance, and UV-resistance. Optically transparent materials that are resistant to UV light have attracted considerable attention because of their important practical applications. Previously, we reported that trifluoropropyl-substituted CO-POSS-pendant polysiloxanes exhibited UV-resistant optically transparent materials. The present study shows that phenyl-substituted CO-POSS-pendant polysiloxanes are alternative UV-resistant, optically transparent materials with higher heat resistance. Whereas the flexibility of **PolyPh-H<sup>b</sup>** was relatively low, the film of **PolyPh-V** could be bent without cracking, it was lightweight, and it exhibited high heat resistance. However, a lower  $T_g$  and reduced UV resistance were observed. This study is expected to contribute to a better understanding of silicone materials, where the relationship between molecular-level structure and bulk properties is unknown. The present study will aid in the fabrication of optically transparent materials that combine several trade-off properties, such as thermal insulation, heat resistance, UV resistance, flexibility, high refractive index, and light weight characteristics.

## Experimental

### Materials

All solvents and chemicals were of reagent-grade quality and used without further purification. Tetrahydrofuran (super dehydrated, stabilizer-free) was purchased from Fujifilm Wako Chemicals U.S.A. Corporation. 3,7,14-Tris(dimethylsilylsiloxy)heptaphenyltricycloheptasiloxane (**Ph-H**) and 3,7,14-tris(dimethylvinylsilylsiloxy)heptaphenyltricycloheptasiloxane (**Ph-V**) were prepared according to a previous report<sup>24</sup> from heptaphenyl-trisilanol-POSS, which were purchased from Hybrid Plastics Inc., (Hattiesburg, Mississippi, US). Tris(dimethoxysilyl-ethyl-dimethylsiloxy)-heptatrifluoropropyl-substituted open-cage silsesquioxane (**F-H**) and tris(dimethoxysilyl-ethyl-dimethylsiloxy)-heptaisobutyl-substituted open-cage silsesquioxane (**B-H**) was prepared according a previous report.<sup>18</sup> Dimethylmethoxyvinylsilane was prepared from chlorodimethylvinylsilane and methanol in 4-methyltetrahydropyran with imidazole and purified by distillation (Fig. S12†). Its boiling temperature was similar to that reported data, 80–85 °C.<sup>25</sup> 1-(Methyldimethoxysilyl)-2-(dimethylmethoxysilyl)ethane (MDME) was prepared by hydrosilylation from dimethoxymethylsilane and dimethylmethoxyvinylsilane (Fig. S13†).

### Instruments

A Bruker AVANCE II 600 spectrometer was used to obtain solid-state  $^{13}C$  (150 MHz) and  $^{29}Si$  (119 MHz) cross-polarization magic angle spinning (CP-MAS) NMR spectra. Fourier transform infrared (FT-IR) spectra were recorded with a JASCO FT/IR-4600 spectrometer (JASCO, Tokyo, Japan). A Jasco spectrophotometer V-670 KKN (Jasco, Tokyo, Japan) was used to record UV-vis spectra. TGA was performed using a Shimadzu DTG-60 Thermogravimetric Analyzer (Shimadzu, Kyoto, Japan) under  $N_2$  or dry air at a heating rate of 10 °C  $min^{-1}$ . DSC was conducted using a Shimadzu DSC-60 Plus. DMA of rectangular samples (20 mm × 9.5 mm × 0.15 mm), which were cut from the cast films, was performed using a DMA7100 (Hitachi High-Tech) instrument at a heating rate of 2 °C  $min^{-1}$  at 1 Hz under  $N_2$  flow. An AccuPyc II 1340 gas displacement pycnometry system (Micromeritics Instrument Corporation, Norcross, CA, USA) was used to obtain density data; the sample was placed in a 0.1 cm<sup>3</sup> chamber and the measured pressure of He was 135 kPa at 25 °C. The thermal diffusivity of the films was measured as a value in the thickness direction using an ai-phase mobile 1u (ai-phase Co. Ltd, Tokyo, Japan) based on the temperature wave analysis method. The specific heat capacity was estimated using a DSC-60 Plus (Shimadzu, Kyoto, Japan) with alumina as the reference substance. The UV irradiation tests were performed under air at room temperature using a UV lamp (365 nm) placed 1 cm from the cast films. Static contact angles of the films were measured at 25 °C using a DMS-301/401 (Kyowa Interface Science, Saitama, Japan) with water (1.0  $\mu$ L) or *n*-tetradecane (1.0  $\mu$ L) as probe fluids. The average of four independent measurements was used for each contact angle. The ultraviolet irradiation test was performed using a UV lamp (365 nm) with a distance of 1 cm to cast films under air at room temperature.

### Synthesis

**Ethylene-linked tris(dimethoxysilyl)-heptaphenyl-substituted open-cage silsesquioxane (Ph-H).** Dimethoxymethylvinylsilane (1.22 mL, 8.14 mmol) and Pt(dvs) (2wt% in xylene, 72.30  $\mu$ L) were added to a solution of **Ph-H** (2.00 g, 1.81 mmol) in superdehydrated toluene (18.0 mL) under  $N_2$ . The reaction mixture was stirred at 80 °C for 6 h. SiliaMetS® triamine metal scavenger (0.50 g) was used to remove the Pt catalyst. After filtration of the reaction mixture, the resulting colorless filtrate was concentrated, dried under vacuum, and purified by HPLC (eluting with  $CHCl_3$ ) to give a colorless viscous liquid (70% yield, 1.89 g, 1.26 mmol).  $^1H$  NMR ( $CDCl_3$ , 400 MHz):  $\delta$  7.53 and 7.40–7.28 and 7.16–7.09 (m, 35H), 3.48–3.43 (m, 18H), 1.14–1.12 and 0.53 (m, 12H), 0.35–0.27 (m, 18H), 0.11–0.03 (m, 9H) ppm.  $^{29}Si$  NMR ( $CDCl_3$ , 80 MHz):  $\delta$  12.43, 12.37, –0.61, –77.41, –77.81, –78.04, –78.10 ppm.  $^{13}C$  NMR ( $CDCl_3$ , 100 MHz):  $\delta$  134.00, 133.98, 133.93, 127.56, 127.54, 127.51, 127.47, 77.34, 77.03, 76.71, 50.15, 8.82, 4.14, –0.40, –0.42, –6.62 ppm. MALDI-TOF-MS ( $m/z$ ): calcd for  $C_{63}H_{92}O_{18}Si_{13}Na$  [ $M + Na$ ]<sup>+</sup>: 1523.3182; found: 1523.3070.



**Propylenethioethyl-linked tris(dimethoxysilyl)-heptaphenyl-substituted open-cage silsesquioxane (Ph-V).** To a solution of **Ph-V** (2.00 g, 1.69 mmol) and AIBN (27.71 mg, 0.17 mmol) in a super-dehydrated toluene (9.38 mL) was added 3-mercaptopropyl(dimethoxy)methylsilane (1.36 mL, 7.56 mmol) under N<sub>2</sub> and the reaction mixture was stirred at 80 °C overnight. The solvent was removed under reduced pressure then the resulting liquid was dried under vacuum and further purified by HPLC (eluting with CHCl<sub>3</sub>) to give a colorless viscous liquid (62% yield, 1.81 g, 1.05 mmol). <sup>1</sup>H NMR (CDCl<sub>3</sub>, 400 MHz): δ 7.54–7.53 and 7.38–7.26 and 7.18–7.09 (m, 35H), 3.50 (s, 18H), 2.55–2.50 (m, 6H), 2.44–2.41 (t, *J* = 8.0, 4.0 Hz 6H), 1.59–1.56 (m, 6H), 1.00–0.96 (m, 6H), 0.70–0.66 (m, 6H), 0.32–0.29 (m, 18H), 0.11 (s, 9H) ppm. <sup>29</sup>Si NMR (CDCl<sub>3</sub>, 80 MHz): δ 10.27, –1.66, –77.35, –77.54, –77.91 ppm. <sup>13</sup>C NMR (CDCl<sub>3</sub>, 100 MHz): δ 133.98, 133.92, 133.87, 127.65, 127.59, 77.34, 77.03, 76.71, 50.19, 35.16, 26.72, 22.99, 18.88, 12.68, 0.43, –5.75 ppm. MALDI-TOF-MS (*m/z*): calcd for C<sub>72</sub>H<sub>110</sub>S<sub>3</sub>O<sub>18</sub>Si<sub>13</sub>Na [M + Na]<sup>+</sup>: 1745.3753; found: 1745.3868.

### Film preparation

To a solution of **Ph-H** (0.25 g, 0.17 mmol) in THF (6.47 mL) was added distilled water (0.40 mL) and 1 M HCl (0.023 mmol) and the resulting solution was stirred at 0 °C for 0.5 h and at room temperature for 3 h to allow hydrolysis and partial condensation. The reaction mixture was then concentrated under vacuum and re-dissolved in THF (2 mL), followed by filtering through a 0.45 μm PTFE syringe filter. The solution was cast onto a clean quartz substrate or a PTFE sheet, air-dried at room temperature for one or two days to remove the most of the solvents, and heated at either 50 °C for 6 h for **PolyPh-H<sup>b</sup>** or 100 °C for 6 h for **PolyPh-H<sup>c</sup>**. To prepare **PolyPh-H<sup>a</sup>**, the residues obtained after the hydrolysis of **Ph-H** under the same conditions used to prepare **PolyPh-H<sup>b</sup>** and **PolyPh-H<sup>c</sup>** described above, was re-dissolved in THF (1.56 mL) and heated at 50 °C for 6 h.

Random polysiloxanes were prepared from MDMS and phenyltrimethoxysilane (PTMS) at a molar ratio of 3 : 7 under the same conditions used for **1**. The reaction solutions were concentrated under vacuum and the resulting residue was redissolved in THF (1.56 mL). The solution was drop-cast onto a clean quartz substrate or a PTFE sheet. The samples were air-dried at room temperature for 1 d to remove the most of the solvents and heated at either 50 °C for 6 h (**Ran-A**) or 110 °C for 6 h (**Ran-B**).

### Author contributions

M. Kosaka: synthesis, measurement, data curation; K. Kanaori: measurement, data curation, review and editing; H. Imoto: conceptualization, investigation, writing – review and editing, supervision; K. Naka: conceptualization, investigation, writing – original draft, writing – review and editing, funding acquisition project administration, supervision.

### Data availability

The authors confirm that the data supporting the findings of this study are available within the article and its ESI.†

Raw data were generated at Kyoto Institute of Technology. Derived data supporting the findings of this study are available from the corresponding author on request.

### Conflicts of interest

There are no conflicts to declare.

### Acknowledgements

This work was supported by Grant-in-Aid for Scientific Research (No. 19H02764 and 23K17944) from the Ministry of Education, Culture, Sports, Science, and Technology, Government of Japan. We thank Prof. Tsuyoshi Kawai, Ms Yoshiko Nishikawa, and Ms Mieko Yamagaki of Nara Institute of Science and Technology for performing MALDI-TOF-MS supported by ARIM.

### References

- 1 A. M. Sawvel, J. C. Crowhurst, H. E. Mason, J. S. Oakdale, S. Ruelas, H. V. Eshelman and R. S. Maxwell, *Macromolecules*, 2021, **54**, 4300–4312.
- 2 C. Robeyns, L. Picard and F. Ganachaud, *Prog. Org. Coat.*, 2018, **125**, 287–315.
- 3 J.-Y. Bae, H.-Y. Kim, Y.-W. Lim, Y.-H. Kim and B.-S. Bae, *RSC Adv.*, 2016, **6**, 26826–26834.
- 4 J.-S. Kim, S.-C. Yang and B.-S. Bae, *Chem. Mater.*, 2010, **22**, 3549–3555.
- 5 J.-Y. Bae, H.-Y. Kim, Y.-B. Kim, J. Jin and B.-S. Bae, *ACS Appl. Mater. Interfaces*, 2015, **7**, 1035–1039.
- 6 H. R. Fischer, C. Semprimoschnig, C. Mooney, T. Rohr, E. R. H. van Eck and M. H. W. Verkuijlen, *Polym. Degrad. Stab.*, 2013, **98**, 720–726.
- 7 H. W. Ro, E. S. Park, C. L. Soles and D. Y. Yoon, *Chem. Mater.*, 2010, **22**, 1330–1339.
- 8 L.-H. Lee, W.-C. Chen and W.-C. Liu, *J. Polym. Sci., Part A: Polym. Chem.*, 2002, **40**, 1560–1571.
- 9 J. H. Lee, W. C. Kim, S. K. Min, H. W. Ree and D. Y. Yoon, *Macromol. Mater. Eng.*, 2003, **288**, 455–461.
- 10 Y. Chujo and K. Tanaka, *Bull. Chem. Soc. Jpn.*, 2015, **86**, 633–643.
- 11 R. M. Laine, *J. Mater. Chem.*, 2005, **15**, 3725–3744.
- 12 D. B. Cordes, P. D. Lickiss and F. Rataboul, *Chem. Rev.*, 2010, **110**, 2081–2173.
- 13 H. Imoto, Y. Nakao, N. Nishizawa, S. Fujii, Y. Nakamura and K. Naka, *Polym. J.*, 2015, **47**, 609–615.
- 14 M. Miyasaka, Y. Fujiwara, H. Kudo and T. Nishikubo, *Polym. J.*, 2010, **42**, 799–803.



- 15 H. Imoto, A. Ishida, M. Hashimoto, Y. Mizoue, S. Yusa and K. Naka, *Chem. Lett.*, 2019, **48**, 1266–1269.
- 16 L. Li, H. Imoto and K. Naka, *J. Appl. Polym. Sci.*, 2021, **138**, 50167.
- 17 T. Nakano, K. Okamoto, H. Imoto and K. Naka, *Polym. J.*, 2023, **55**, 193–201.
- 18 L. Li, H. Imoto, A. Okada, K. Kanaori and K. Naka, *ACS Appl. Polym. Mater.*, 2021, **3**, 1368–1375.
- 19 M. Kosaka, T. Nakano, K. Kanaori, H. Imoto and K. Naka, *Polym. J.*, 2024, **56**, 481–489.
- 20 A. Fina, D. Tabuani, F. Carniato, A. Frache, E. Boccaleri and G. Camino, *Thermochim. Acta*, 2006, **440**, 36–42.
- 21 Z. Zhang, B. P. Gorman, H. Dong, R. A. Orozco-Teran, D. W. Mueller and R. F. Reidy, *J. Sol-Gel Sci. Technol.*, 2003, **28**, 159–165.
- 22 T. B. Casserly and K. K. Gleason, *J. Phys. Chem. B*, 2005, **109**, 13605–13610.
- 23 A. J. Guenther, K. R. Lamison, L. M. Lubin, T. S. Haddad and J. M. Mabry, *Ind. Eng. Chem. Res.*, 2012, **51**, 12282–12293.
- 24 S. Yuasa, Y. Sato, H. Imoto and K. Naka, *Bull. Chem. Soc. Jpn.*, 2019, **92**, 127–132.
- 25 P. R. Jones, T. F. O. Thomas, M. L. McBee and R. A. Pierce, *J. Organomet. Chem.*, 1987, **159**, 99–110.

